Chemical and Biological Engineering Publications   Chemical and Biological Engineering

2006

Modeling styrene-styrene interactions

Ivana Adamovic
Iowa State University

Hui Li
Iowa State University

Monica H. Lamm
Iowa State University, mhlamm@iastate.edu

See next page for additional authors

Follow this and additional works at: http://lib.dr.iastate.edu/cbe_pubs

Part of the Biochemical and Biomolecular Engineering Commons

The complete bibliographic information for this item can be found at http://lib.dr.iastate.edu/cbe_pubs/187. For information on how to cite this item, please visit http://lib.dr.iastate.edu/howtocite.html.

Modeling styrene-styrene interactions

Abstract

This study is the first step in the systematic investigation of substituted (carboxyl) polystyrene nanoparticles. Understanding the fundamental interactions between the p-carboxyl styrene monomers, where an ethyl group is used instead of a vinyl group (referenced, for convenience, as "p-carboxyl styrene"), provides the basic information needed to construct potentials for nanoparticles composed of these monomers. In this work, low-energy isomers of p-carboxyl styrene dimer were studied. The dimer structures and their relative and binding energies were determined using both MÃ¸ller-Plesset second-order perturbation theory (MP2) and the general effective fragment potential (EFP2) method. Sections of the intermolecular potential energy surface (PES) of the p-carboxylated styrene dimer in its global minimum orientation were also determined. As expected, double hydrogen bonding between the two carboxylic groups provides the strongest interaction in this system, followed by isomers with a single H-bond and strong benzene ring-benzene ring (Ï€-Ï€) type interactions. Generally, the EFP2 method reproduces the MP2 geometries and relative energies with good accuracy, so it appears to be an efficient alternative to the correlated ab initio methods, which are too computationally demanding to be routinely used in the study of the more-complex polymeric systems of interest.

Keywords

ethyl group, modeling, vinyl group, enzene, binding energy, dimers, hydrogen bonds, monomers, nanostructured materials, perturbation techniques, polystyrenes, styrene

Disciplines

Biochemical and Biomolecular Engineering | Chemical Engineering

Authors

Ivana Adamovic, Hui Li, Monica H. Lamm, and Mark S. Gordon

Modeling Styrene−Styrene Interactions[†]

Ivana Adamovic,[‡] Hui Li,[‡] Monica H. Lamm,[§] and Mark S. Gordon*,[‡]

Departments of Chemistry and Chemical and Biological Engineering, Iowa State University, Ames, Iowa 50011

Received: April 27, 2005

This study is the first step in the systematic investigation of substituted (carboxyl) polystyrene nanoparticles. Understanding the fundamental interactions between the *p*-carboxyl styrene monomers, where an ethyl group is used instead of a vinyl group (referenced, for convenience, as "*p*-carboxyl styrene"), provides the basic information needed to construct potentials for nanoparticles composed of these monomers. In this work, low-energy isomers of *p*-carboxyl styrene dimer were studied. The dimer structures and their relative and binding energies were determined using both Møller−Plesset second-order perturbation theory (MP2) and the general effective fragment potential (EFP2) method. Sections of the intermolecular potential energy surface (PES) of the *p*-carboxylated styrene dimer in its global minimum orientation were also determined. As expected, double hydrogen bonding between the two carboxylic groups provides the strongest interaction in this system, followed by isomers with a single H-bond and strong benzene ring−benzene ring ($\pi-\pi$) type interactions. Generally, the EFP2 method reproduces the MP2 geometries and relative energies with good accuracy, so it appears to be an efficient alternative to the correlated ab initio methods, which are too computationally demanding to be routinely used in the study of the more-complex polymeric systems of interest.

I. Introduction

It is common knowledge that nanoparticles exhibit different— and, often, more useful—properties than those of bulk material. Although nanoparticle syntheses based on empirical methods have existed for many years, very few synthesis strategies have been developed based on fundamental knowledge of the chemistry and physics involved.[1] Many applications for nano-particles in pharmaceuticals, coatings, and catalysis require stable particle dispersions with uniform size distribution, which, in turn, require a detailed understanding of the nanoparticle−nanoparticle interactions that drive aggregation.[2−5] In particular, the long-term goal of this effort is to predict aggregation properties as a function of nanoparticle surface chemistry. Carboxylated polystyrene latex nanoparticles have been chosen as a model system for this study, because of the relative ease with which the surface coverage of the carboxylic acid can be controlled in experiments.[6] These particles are used in im-munological,[7,8] drug delivery,[9−11] and heterogeneous catalysis[12] applications, because the presence of the carboxylic acid functionality promotes the binding of antibodies, proteins, and metals to the latex particle surface. As an initial step toward the theoretical prediction of both polymer aggregation mecha-nisms in general and carboxylated polystyrene latex nanopar-ticles in particular, the present work initiates a systematic investigation of the fundamental interactions in *p*-carboxyl polystyrene nanoparticles, by studying the simplest prototype of such nanoparticle-nanoparticle interactions: *p*-carboxyl sty-rene dimer.

Surprisingly, a literature search for substituted styrene dimers revealed no studies with a focus on the fundamental interactions in these systems. On the other hand, there have been many experimental and theoretical studies on the styrene monomer itself. The majority of that work is concerned with the geometry of the styrene monomer in its ground electronic state, primarily the issue of its planarity versus nonplanarity.[13] Theoretical studies are equally divided between those supporting a planar structure versus a twisted structure. A detailed overview of theoretical and experimental studies on the torsional potential of styrene is given in ref 6. All ab initio methods—Hartree−Fock (HF), Møller−Plesset second-order perturbation theory (MP2), and coupled cluster (CC)—agree that the twisted structure is the global minimum, whereas density functional theory (DFT) studies indicate that the lowest energy minimum is planar. However, all ab initio calculations predict the twisted structure to be <1 kcal/mol lower in energy than the planar form, so even the inclusion of zero-point vibrational and temperature effects could change the result in favor of the planar structure. Most experimental studies have concluded that, in the ground electronic state, the styrene monomer is planar.[14,15]

An ab initio (HF and configuration interaction singles (CIS), with MP2 correction) study by Zilberg and Hass[16] described the vibrational spectra of the ground and first excited singlet states of styrene and β-methyl styrene. It was found that the ground state of the molecule has a broad shallow torsional potential. A theoretical study of the electronic spectra of styrene was reported by Molina et al.,[17,18] with a specific focus on the cis−trans photoisomerization. The vertical singlet−triplet elec-tronic spectrum of styrene was considered in a theoretical study by Wan and Nakatsuji.[19]

Binary clusters composed of styrene monomer and polar (methanol[20] or water[21]) clusters were extensively studied by the resonant two-photon ionization technique. These studies pro-posed a proton-transfer reaction, from the styrene dimer cation to water or methanol cluster, as a possible cause of the inhibition mechanism observed in the cationic polymerization of styrene.

As can be seen from this brief literature overview, there have been several studies of the styrene monomer, but there has been little or no analysis of the fundamental interactions in the styrene dimer. Cationic benzene clusters were studied using both experimental and theoretical means, by El-Shall and co-

---

* Author to whom correspondence should be addressed. Telephone: 515-294-0452, -6342. Fax: 515-294-0105, -5204. E-mail address: mark@ si.fi.ameslab.gov, gordon@ameslab.gov.
‡ Department of Chemistry.
§ Department of Chemical and Biological Engineering.

workers.[22] For the purpose of this study, the most relevant work is the analysis of neutral benzene and substituted benzene dimers by Sherrill and co-workers.[23−26] More details on these studies follow in Section III.A.

The major goal of this work is to shed more light on the fundamental interactions that govern the formation and aggregation of substituted styrene nanoparticles. As a first step in this direction, the low-energy structures of the dimer of *p*-carboxyl styrene are presented. The most important intermolecular interactions have been determined and the ability of the general effective fragment potential (EFP2) method to adequately represent the *p*-carboxyl styrene dimer PES is discussed.

This work is organized as follows: Section II gives a brief overview of the EFP2 method, followed by the computational details in Section III, results and discussion in Section IV, and general conclusions in Section V.

II. Theoretical Methods−General Effective Fragment Potential (EFP2)

The general effective fragment potential (EFP) is a discrete solvation method that is based on fundamental quantum mechanics. Because the method contains no empirically fitted parameters, the EFP2 approach is generally applicable in the sense that an EFP can be generated for *any* chemical species for which one can perform the "MAKEFP" calculation in GAMESS,[27] in which all contributions to the EFP2 interaction potential for the desired species are generated automatically in a single ab initio run. Current applications of EFP2 include the study of Ar clusters and water−alcohol mixtures.[28] A detailed description of the EFP2 method is given elsewhere;[29] hence, only a brief overview of the method is given here.

The EFP2 potential contains several terms that represent most of the physically meaningful intermolecular interactions that a molecular species can experience. Each of these terms can represent EFP−EFP interactions or effective fragment potential−quantum mechanics (EFP−QM) interactions, where the QM portion of the system of interest would typically describe a solute in the presence of an EFP solvent. The focus in the present work is only on EFP−EFP interactions.

In the present implementation, the interaction potential *V* includes electrostatic (Coulomb), induction (polarization), exchange repulsion, and dispersion energy contributions.

Coulomb Interaction. The electrostatic potential is represented using a distributed multipolar analysis (DMA).[30,31] The molecular density is represented by an expansion up through octopole moments, with the expansion centers at the atom nuclei and bond midpoints. Because the DMA is a classical pointwise model, it cannot account for the actual quantum mechanical overlap of two charge densities that would occur at short fragment−fragment distances. These charge penetration effects are accounted for by multiplying the charge−charge portion of the mutipole expansion by a distance-dependent cut-off function.[32]

Induction (Polarization) Energy. Induction energy is treated in a self-consistent manner, using localized molecular orbitals[33,34] (LMOs). First, the total polarizability tensor is expressed as a sum of the LMO polarizabilities of bonds and lone pairs. Coupled perturbed Hartree−Fock calculations are then used to calculate LMO polarizability tensors. After the distributed polarizability components have been determined, the polarization (induction) energy is iterated to self-consistency.

Exchange Repulsion Energy. As shown previously,[29,35−37] the exchange repulsion energy can be expanded in three distinct energy terms, based on their explicit dependence on the *intermolecular* overlap:

$$E_{exch}[O(S^2)] \approx E_{exch}[V;O(S^2)] =$$
$$E_{exch}(S^0) + E_{exch}(S^1) + E_{exch}(S^2) \quad (1)$$

The required intermolecular overlap integrals are computed using LMOs whose linear combination of atomic orbitals (LCAO) coefficients are fixed, but whose orientations in space can vary as the fragments move relative to each other. The use of localized orbitals in this manner means that the expansion in the intermolecular overlap can be truncated at the quadratic term, as indicated in eq 1.[36,37]

Dispersion Energy. In the EFP2 method, a standard series expansion of the fragment−fragment dispersion energy[38] in terms of $1/R^n$ (n = 6, 8, ...) is used:[30]

$$E_{disp} = \frac{C_6}{R^6} + \frac{C_8}{R^8} + \frac{C_{10}}{R^{10}} + ... \quad (2)$$

These respective terms correspond physically to induced dipole−induced dipole, induced dipole−induced quadrupole, induced quadrupole−induced quadrupole, etc., interactions. In the current implementation, the series expansion is terminated at the first (dipole−dipole) term, with an approximate estimate for the higher-order terms. As for the polarizability and exchange repulsion interactions, the C_6 coefficients are obtained by making use of LMOs. In particular, a C_6 coefficient is determined for each pair of LMOs *i* and *j*. These LMO dispersion coefficients are determined by numerical integration of products of dynamic polarizabilities, over a range of imaginary frequencies. These LMO dispersion coefficients are then summed to obtain a fragment−fragment dispersion coefficient, C_6. The $R^{−8}$ term is estimated as a fraction of the $R^{−6}$ term. Expression 2 is also corrected for short-range charge penetration effects, by multiplying it by an appropriate damping function.[38]

III. Computational Details

All of the calculations presented here were performed with the electronic structure code GAMESS.[27] The first step in this study was to generate an EFP2 potential for *p*-carboxyl styrene monomer, in its MP2//aug-cc-pVDZ[39] optimized geometry. To simulate the polymer environment, an ethyl group, rather than a vinyl group, was placed on the benzene ring. All energy terms described previously, except the electrostatic interaction, were generated using the 6-31+G(d) basis set.[40,41] The DMA for the Coulomb energy term was generated with the 6-31G(d)[40,41] basis set. As has been noted by other researchers,[42] the generation of multipole moments for benzene-like molecules, using basis sets that use diffuse functions, can lead to nonphysical values for the charges and higher multipoles, because of linear dependences in the basis set.

Location of global minima on the dimer surface was accomplished by Monte Carlo/simulated annealing simulations,[43−45] using the EFP2 method. More details about these calculations will be given in Section IV. Second-order perturbation theory (MP2)[46] geometry optimizations were also performed for several low-energy isomers using the 6-31+G(d)[40,41] basis set. In these MP2 optimizations, the internal geometries were fixed at the monomer geometries for compatibility with the EFP2 method, because the EFP2 internal structures are frozen. Single-point
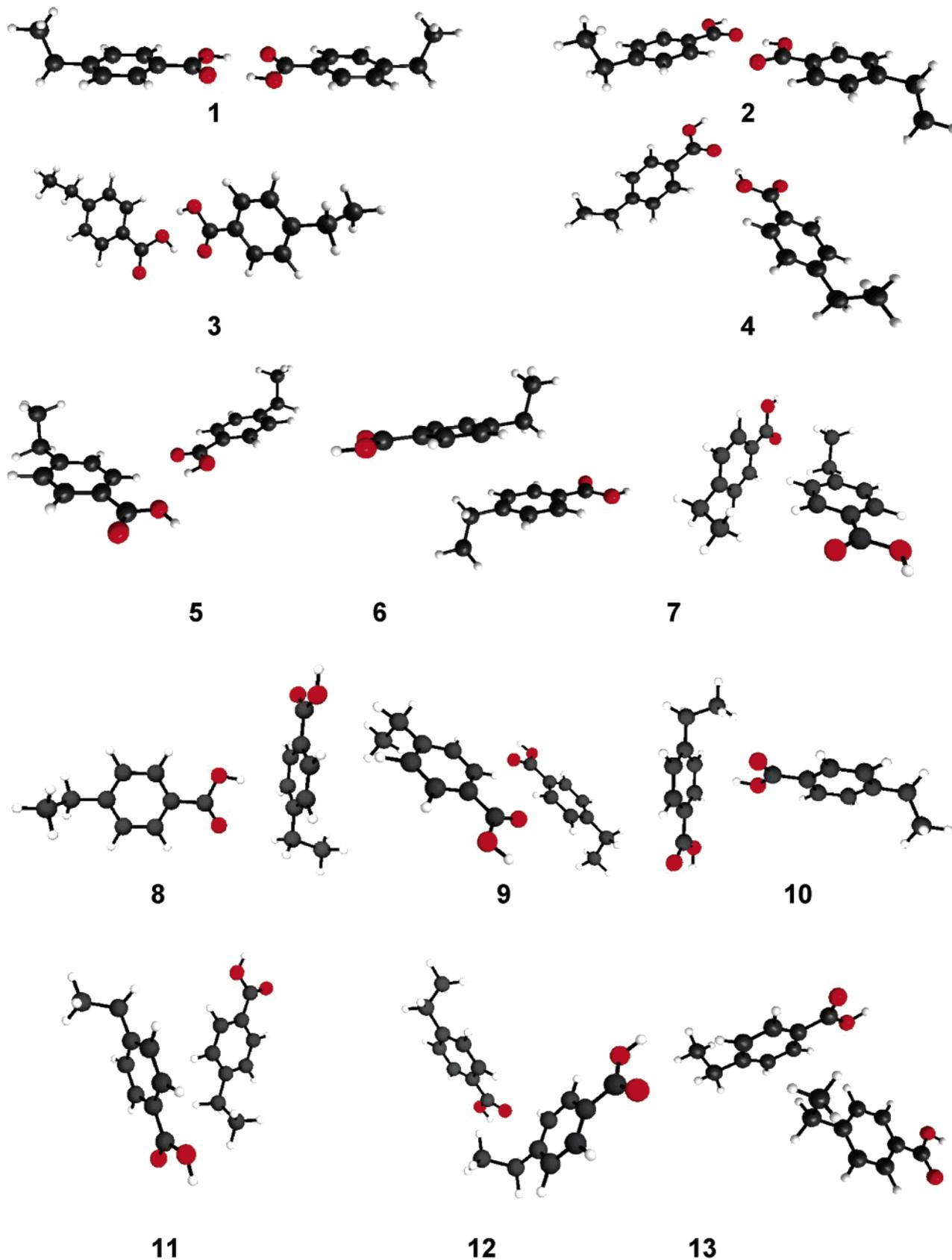
Figure 1. Lowest-energy isomers for the *p*-carboxyl styrene dimer.

MP2 energy calculations were performed at all EFP2 local minimum structures. Sections of the potential energy surface have also been determined with MP2 calculations. EFP2 Hessians (energy second derivatives) were performed to ensure that stationary points are, indeed, local minima.

IV. Results and Discussion

IV. A. Low-Energy Minima of *p*-Carboxyl Styrene (COOH−PhC$_2$H$_5$) Dimer. The major interaction in the dimer of *p*-carboxyl styrene is hydrogen bonding. The presence of the

522 *J. Phys. Chem. A, Vol. 110, No. 2, 2006*

Adamovic et al.

TABLE 1: Binding Energies for Lowest-Energy Isomers of *p*-Carboxyl Styrene Dimer

	Binding Energy (kcal/mol)	
isomer	MP2//6-31+G(d)	EFP2
1	15.8	14.7
2	9.3	7.7
3	8.6	7.1
4	7.8	6.1
5	6.9	4.5
6	9.8	3.9
7	8.1	3.8
8	7.3	3.8
9	5.1	3.7
10	7.6	3.6
11	7.8	3.4
12	5.6	3.0
13	6.9	2.7

TABLE 2: Relative Energies for Lowest-Energy Isomers of *p*-Carboxyl Styrene Dimer

	Relative Energy (kcal/mol)	
isomer	MP2//6-31+G(d)[a]	EFP2
1	0.0	0.0
2	6.5 (6.3)	7.0
3	7.2 (6.9)	7.6
4	7.9 (6.7)	8.6
5	8.8	10.2
6	5.9	10.8
7	7.6	10.9
8	8.5	10.9
9	10.6	10.9
10	8.1	11.1
11	7.9	11.3
12	10.2	11.6
13	8.9	12.0

[a] Results in parentheses are MP2 constrained optimizations.

−COOH groups introduces the possibility of double O−H···O═ hydrogen bond formation, which is expected to provide more stability than other types of interactions between two *p*-carboxyl styrene monomers. To explore all possible dimer arrangements, Monte Carlo/simulated annealing (MC/SA) EFP2 calculations were performed starting from different initial geometries and simulation conditions. MC/SA calculations were performed using an initial temperature in the range of 1000−500 K. The EFP2 *p*-carboxyl styrene monomers were allowed to move in a box size of 10 Å × 10 Å × 10 Å. Geometry optimizations were performed every 50, 80, and 100 steps. These simulations resulted in the lowest-energy dimer structures shown in Figure 1. Although the MC/SA searches were extensive, it is, of course, possible that there are some other low-energy dimer structures that have not been found.

EFP2 and MP2 binding energies (with respect to separated monomers) for 13 lowest-energy isomers are given in Table 1, whereas relative energies (with respect to the lowest-energy isomer) are given in Table 2. The EFP2 and MP2 global minimum on the dimer surface is isomer **1**, which is a structure with two hydrogen bonds. Both levels of theory predict this structure to be ∼5 kcal/mol more stable than the next lowest-energy structure. With just a few exceptions, the EFP2 energy ordering of the 13 isomers is in very good agreement with the MP2 relative energies. For example, the first four entries in Table 2 are in the same order and the binding energy differences are <1 kcal/mol (see Table 1). Note that constrained MP2 optimizations on the four lowest-energy isomers (shown in parentheses in Table 2) have a small effect on the relative energies. A few of the higher-energy isomers differ in relative

TABLE 3: Energy Decomposition for the Six Lowest-Energy Isomers

	Energy Decomposition (kcal/mol)				
isomer	electrostatic	repulsion	polarization	dispersion	total
1	−17.6	12.7	−6.8	−3.1	−14.7
2	−8.1	4.4	−1.7	−2.2	−7.7
3	−8.4	5.7	−2.2	−2.2	−7.1
4	−6.4	3.7	−1.5	−1.9	−6.1
5	−4.8	3.3	−0.8	−2.1	−4.5
6	−0.5	2.9	−0.2	−6.1	−3.9

energies by 1−3 kcal/mol, with the largest disagreement of ∼5 kcal/mol for isomer **6**.

The disagreement between EFP2 and MP2 for the relative energy and binding energy of isomer **6** is somewhat surprising, in view of the much better agreement for the other isomers. Because the EFP2 method is independent of MP2, it is not obvious which method is closer to the correct binding energy. Although coupled cluster calculations with a reliable basis set on the substituted styrene dimer are currently too computationally demanding, some insight can be gained from previous MP2 and CCSD(T) calculations on substituted benzene dimers by Sherrill and co-workers.[8−11] Because the major portion of the interaction energy in isomer **6** comes from the benzene ring π−π interaction, the accuracy of MP2, relative to CCSD(T), can be used to assess the MP2 performance for the π-stacked styrene dimer. The general conclusion drawn by Sherrill et al. is that, at the equilibrium geometry, the MP2 binding energies for π-stacked interactions overestimate the more-accurate CCSD(T) values by ∼2.0 kcal/mol (∼40% of the total binding energy), when the aug-cc-pVQZ basis set is used. These results on benzene dimers suggest that MP2 overestimates the π-stacked interaction energy in the substituted styrene dimers of interest here by ∼4 kcal/mol (if the same percent error is used), whereas EFP2 then underestimates this π-stacked binding energy by ∼2 kcal/mol. Of course, this analysis is approximate, but it does suggest that the EFP2 method provides an accuracy for weak π-stacked interactions that is comparable to that of the much more computationally demanding MP2 method. EFP2 may underestimate the dispersion interaction, because of the neglect of higher-order terms in the series expansion.

The EFP2 interaction energies for the six lowest-energy isomers are decomposed into their component contributions in Table 3. The electrostatic interaction is, by far, the most important source of binding for the five lowest-energy isomers. These five isomers contain two hydrogen bonds (isomer **1**) or one hydrogen bond (isomers **2**−**5**), so the importance of the Coulomb interaction is not surprising. For these five isomers, the relative size of the exchange repulsion interaction approximately mirrors that of the Coulomb interaction, with the opposite sign. The same is true for the polarization interaction. For all of these isomers, the dispersion contribution is small but nontrivial. For the stacked π-system of benzene rings in isomer **6**, dispersion is the dominant interaction at ∼6 kcal/mol.

IV.B. Potential Energy Surface for Global Minimum *p*-Carboxyl Styrene Dimer. In this section, the potential energy surface (PES) corresponding to the variation of the interdimer distance is examined for isomer **1**, as a function of the relative orientations of the two monomers. The purpose of this study is to explore how the interdimer energy is dependent on the variation of key interdimer coordinates. The PES was constructed using the MP2//6-31+G(d) method. First, the monomer geometry was optimized at the MP2//aug-cc-pVDZ[39,47] level of theory. After the monomer geometry is determined, it is kept
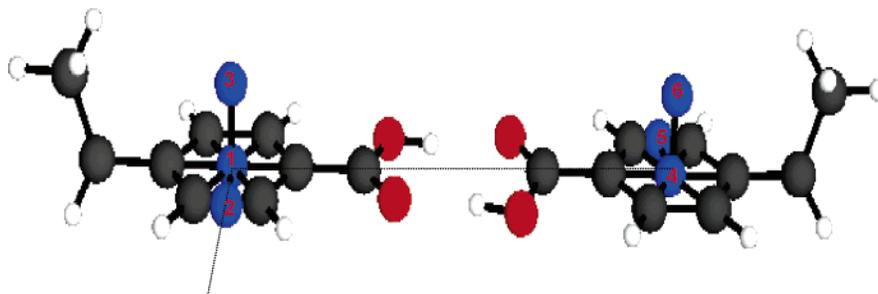
Modeling Styrene−Styrene Interactions

J. Phys. Chem. A, Vol. 110, No. 2, 2006 **523**

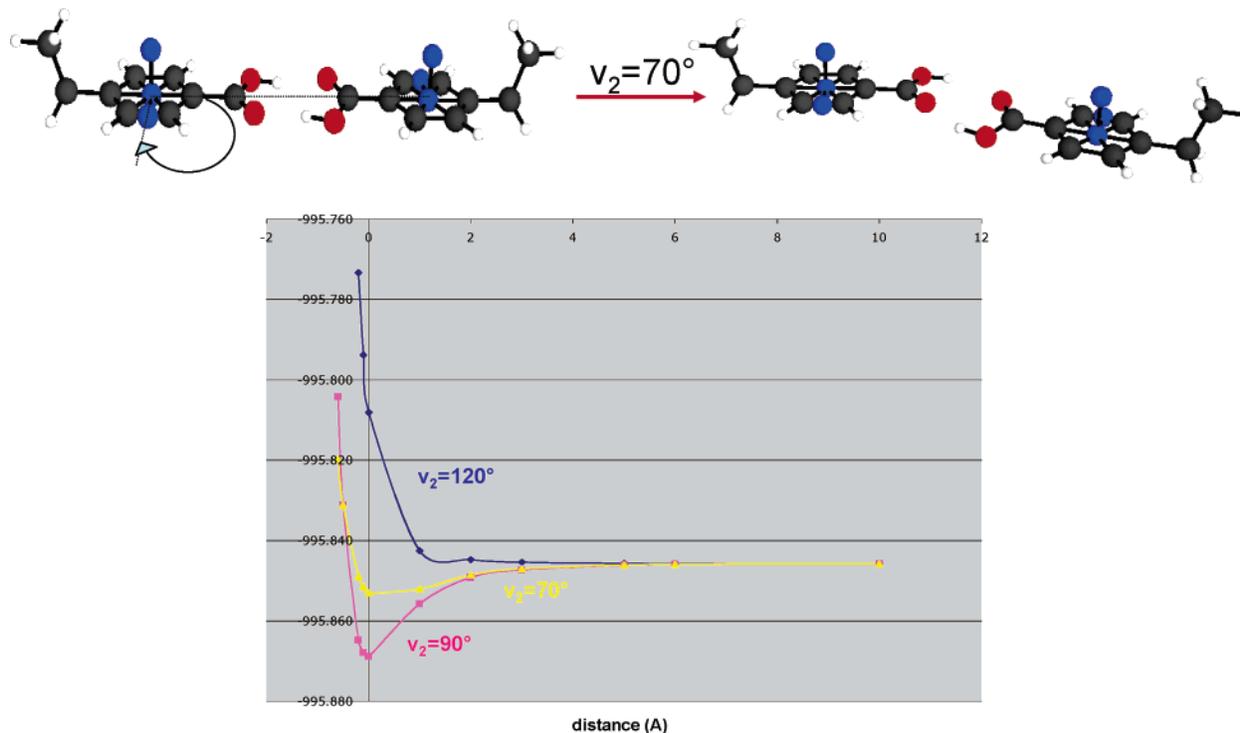**Figure 2.** Internal coordinate system for the potential energy surface (PES) construction.

Figure 3. PES for internal coordinate v_2 (energy given in a.u. units, distance given in angstroms).

internally frozen and the optimization of dimer **1** is performed at the MP2//6-31+G(d) level of theory.

To construct the *p*-carboxyl styrene dimer PES, a coordinate system is defined using three points in each monomer, thereby providing six internal coordinates (see Figure 2): the distance (v_1) between the centers of mass of the two monomers, two angles (v_2 = angle 4−1−2 (see Figure 2) and v_4 = angle 3−4−5) and three dihedral angles (v_3 = dihedral angle 4−1−2−3, v_5 = dihedral angle 1−3−4−5, and v_6 = dihedral angle 1−5−4−6).

For the construction of the PES, one of the six internal coordinates was displaced from its equilibrium value, with all others remaining fixed. MP2 single-point energies then were calculated for a range of distances v_1. Figure 3 illustrates cuts of the PES for v_2 = 70°, 90° (equilibrium value), and 120°. The distance v_1 was varied from −0.6 Å (pushing the monomers toward each other from the equilibrium geometry) to 10 Å. Changing the angle v_2 from its equilibrium value to 70° (or 120°) breaks the linearity of the hydrogen-bonded network, so the energy changes dramatically (~10 kcal/mol at 70° and ~15 kcal/mol at 120°). This illustrates the importance of maintaining the linearity of these strong hydrogen bonds. Similar calculations were performed for all other internal coordinates; the final PESs are shown in Figure 4. In each case, v_1 is varied for various displaced values of one of the other internal coordinates. After

the linearity of these hydrogen bonds has been disrupted, the depth of the potential energy wells decreases considerably, because the strength of the hydrogen bonds has now been significantly diminished. Beyond ~4 Å, there is no change in energy for any of the internal coordinates; therefore, a distance of ~4 Å seems to be the extent of the hydrogen-bonding interaction. The PES shown in Figures 3 and 4 illustrates the importance of including a directional hydrogen-bonding term, as well as angular and torsional terms, in any lower-resolution intermolecular potential model that might be constructed to simulate the behavior of several thousands of *p*-carboxyl monomers that interact in polystyrene nanoparticles.

V. Conclusions

This work is a first step in the systematic study of *p*-carboxyl polystyrene nanoparticles. Binding energies and relative energies for a set of 13 low-energy dimer isomers, obtained with the aid of extensive Monte Carlo/simulated annealing calculations, were determined using the MP2 and EFP2 methods. As expected, the most important interaction between two *p*-carboxyl styrene monomers is the formation of a double hydrogen bond, the global minimum on the dimer surface. Other isomers that contain $\pi-\pi$ interactions of benzene rings or single hydrogen bonds are all at least ~5 kcal/mol higher in energy than the

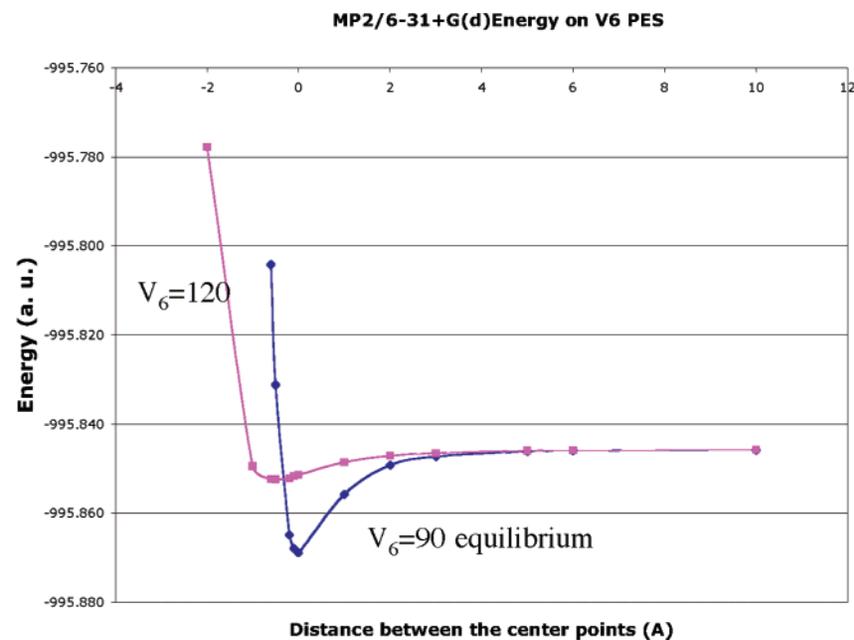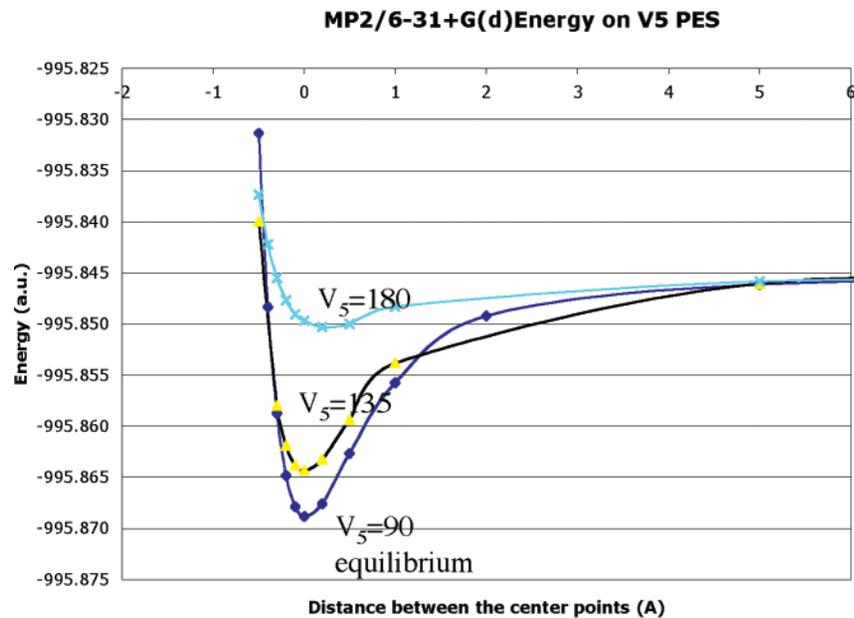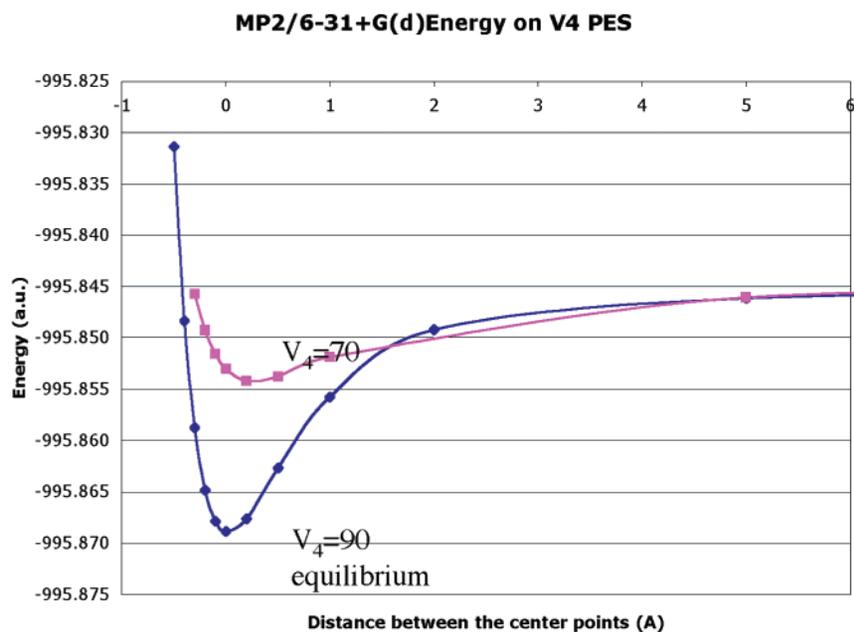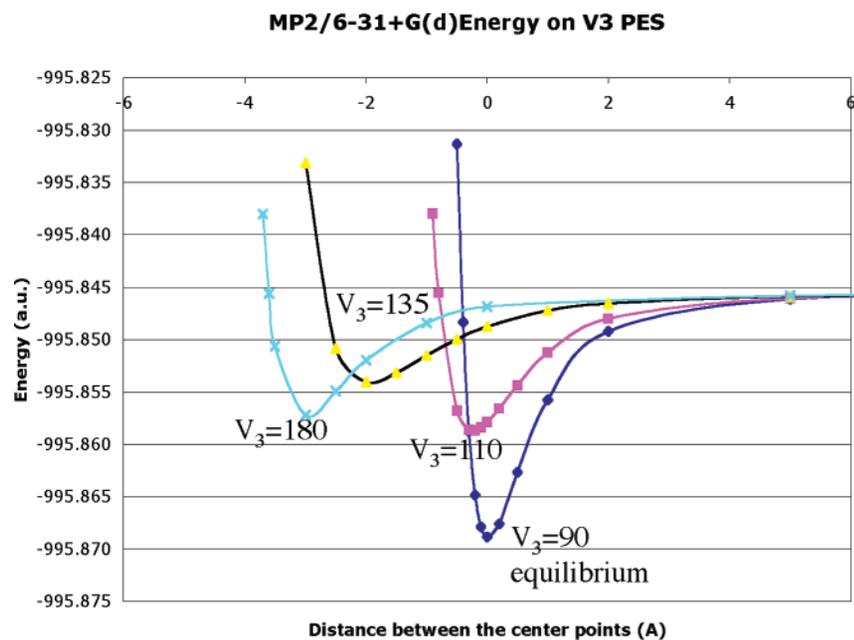**MP2/6-31+G(d)Energy on V3 PES**

MP2/6-31+G(d)Energy on V4 PES

MP2/6-31+G(d)Energy on V5 PES

MP2/6-31+G(d)Energy on V6 PES

Figure 4. PES for internal coordinate v_3, v_4, v_5, and v_6 (energy given in a.u. units, distance given in angstroms).

Modeling Styrene−Styrene Interactions

J. Phys. Chem. A, Vol. 110, No. 2, 2006 **525**

global minimum. The EFP2 and MP2 methods agree reasonably well, with regard to the relative energies of most isomers, with the exception of isomer **6**, for which these two methods predict binding energies that differ by ~6 kcal/mol. Based on comparison with previous CCSD(T) calculations on dimers of substituted benzenes, the MP2 method seems to overestimate the binding energy of π-stacked structures, such as isomer **6**, by ~4 kcal/mol, while EFP2 underestimates the binding energy by ~2 kcal/mol. It is very encouraging that the affordable EFP2 method provides an accuracy for these species that is comparable to that of the much more computationally demanding MP2 method.

The potential energy surface (PES) for the global minimum was studied using the MP2//6-31+G(d) method. The general conclusions of this study are as follows: (i) the dimer PES of *p*-carboxyl styrene is very sensitive, both in terms of angular and torsional dependence, and (ii) for distances of >4 Å, the PES essentially reaches its asymptote, suggesting that the hydrogen-bonding interaction does not extend beyond this distance of ~4 Å.

Based on the results of this study, the newly developed general effective fragment potential (EFP2) method can be used with confidence as an efficient alternative to the MP2 method in studies of *p*-carboxyl polystyrene particles. Future work on this project will focus on constructing potentials for larger *p*-carboxyl fragments using the EFP2 method, with the eventual derivation of a robust force field to be used in simulations of the *p*-carboxyl polystyrene nanoparticles.

References and Notes

(1) Friedlander, S. K. *J. Nanopart. Res.* **1999**, *1*, 159.

(2) Lattuada, M.; Sandkuhler, P.; Wu, H.; Sefcik, J.; Morbidelli, M. *Adv. Colloid Interface Sci.* **2003**, *103*, 33.

(3) Saltiel, C.; Chen, Q.; Manickavasagam, S.; Schadler, L. S.; Siegel, R. W.; Menguc, M. P. *J. Nanopart. Res.* **2004**, *6*, 35.

(4) Sandkuhler, P.; Sefcik, J.; Lattuada, M.; Wu, H.; Morbidelli, M. *AIChE J.* **2003**, *49*, 1542.

(5) Boissier, C.; Loefroth, J.-E.; Nyden, M. *Langmuir* **2002**, *18*, 7313.

(6) Menshikova, A. Y.; Evseeva, T. G.; Skurkis, Y. O.; Tennikova, T. B.; Ivanchev, S. S. *Polymer* **2005**, *46*, 1417.

(7) Wang, P. C.; Lee, C. F.; Young, T. H.; Lin, D. T.; Chiu, W. Y. *J. Polym. Sci., Part A* **2005**, *43*, 1342.

(8) Covolan, V. L.; Mei, L. H. I.; Rossi, C. L. *Polym. Adv. Technol.* **1997**, *8*, 44.

(9) Li, M.; Zhang, Y. B.; Jiang, M.; Zhu, L.; Wu, C. *Macromolecules* **1998**, *31*, 6841.

(10) Olivier, V.; Riviere, C.; Hindie, M.; Duval, J. L.; Bomila-Koradjim, G.; Nagel, M. D. *Colloids Surf. B* **2004**, *33*, 23.

(11) Yamamoto, N.; Fukai, F.; Ohshima, H.; Terada, H.; Makino, K. *Colloids Surf., B* **2002**, *25*, 157.

(12) Dokoutchaev, A.; James, J. T.; Koene, S. C.; Pathak, S.; Prakash, G. K. S.; Thompson, M. E. *Chem. Mater.* **1999**, *11*, 2389.

(13) Sancho-Garcia, J. C.; Perez-Jimenez, A. J. *J. Phys. B: At., Mol. Opt. Phys.* **2002**, *35*, 1509.

(14) Granadino-Roldan, J. M.; Fernandez-Gomez, M.; Navarro, A.; Jayasooriya, U. A. *Phys. Chem. Chem. Phys.* **2003**, *5*, 1760.

(15) Granadino-Roldan, J. M.; Fernandez-Gomez, M.; Navarro, A.; Pena Ruiz, T.; Jayasooriya, U. A. *Phys. Chem. Chem. Phys.* **2004**, *6*, 1133.

(16) Zilberg, S.; Haas, Y. *J. Chem. Phys.* **1995**, *103*, 20.

(17) Molina, V.; Smith, B. R.; Merchan, M. *Chem. Phys. Lett.* **1999**, *309*, 486.

(18) Molina, V.; Merchan, M.; Roos, B. O.; Malmqvist, P.-A. *Phys. Chem. Chem. Phys.* **2000**, *2*, 2211.

(19) Wan, J.; Nakatsuji, H. *Chem. Phys.* **2004**, *302*, 125.

(20) Mahmoud, H.; Germanenko, I. N.; Ibrahim, Y.; El-Shall, M. S. *J. Phys. Chem. A* **2003**, *107*, 5920.

(21) Mahmoud, H.; Germanenko, I. N.; Wright, D.; El-Shall, M. S. *J. Phys. Chem. A* **2005**, *109*, 4474.

(22) Rusyniak, M. J.; Ibrahim, Y. M.; Wright, D. L.; Khanna, S. N.; El-Shall, M. S. *J. Am. Chem. Soc.* **2003**, *125*, 12001.

(23) Sinnokrot, M. O.; Sherrill, C. D. *J. Phys. Chem. A* **2004**, *108*, 10200.

(24) Sinnokrot, M. O.; Sherrill, C. D. *J. Am. Chem. Soc.* **2004**, *126*, 7690.

(25) Sinnokrot, M. O.; Sherrill, C. D. *J. Phys. Chem. A* **2003**, *107*, 8377.

(26) Sinnokrot, M. O.; Valeev, E. F.; Sherrill, C. D. *J. Am. Chem. Soc.* **2002**, *124*, 10887.

(27) Schmidt, M. W.; Baldridge, K. K.; Boatz, J. A.; Elbert, S. T.; Gordon, M. S.; Jensen, J. H.; Koseki, S.; Matsunaga, N.; Nguyen, K. A.; et al. *J. Comput. Chem.* **1993**, *14*, 1347.

(28) Adamovic, I.; Gordon, M. S. Manuscript in preparation.

(29) Gordon, M. S.; Freitag, M. A.; Bandyopadhyay, P.; Jensen, J. H.; Kairys, V.; Stevens, W. J. *J. Phys. Chem. A* **2001**, *105*, 293.

(30) Stone, A. J. *Chem. Phys. Lett.* **1981**, *83*, 233.

(31) Stone, A. J. *The Theory of Intermolecular Forces*; Clarendon Press: Oxford, U.K., 1996.

(32) Freitag, M. A.; Gordon, M. S.; Jensen, J. H.; Stevens, W. J. *J. Chem. Phys.* **2000**, *112*, 7300.

(33) Edmiston, C.; Ruedenberg, K. *Rev. Mod. Phys.* **1963**, *35*, 457.

(34) Raffenetti, R. C.; Ruedenberg, K.; Janssen, C. L.; Schaefer, H. F. *Theor. Chim. Acta* **1993**, *86*, 149.

(35) Jensen, J. H.; Day, P. N.; Gordon, M. S.; Basch, H.; Cohen, D.; Garmer, D. R.; Kraus, M.; Stevens, W. J. *ACS Symp. Ser.* **1994**, *569*, 139.

(36) Jensen, J. H.; Gordon, M. S. *Mol. Phys.* **1996**, *89*, 1313.

(37) Jensen, J. H.; Gordon, M. S. *J. Chem. Phys.* **1998**, *108*, 4772.

(38) Adamovic, I.; Gordon, M. S. *Mol. Phys.* **2005**, *103*, 379.

(39) Dunning, T. H., Jr. *J. Chem. Phys.* **1989**, *90*, 1007.

(40) Hehre, W. J.; Ditchfield, R.; Pople, J. A. *J. Chem. Phys.* **1972**, *56*, 2257.

(41) Francl, M. M.; Pietro, W. J.; Hehre, W. J.; Binkley, J. S.; Gordon, M. S.; DeFrees, D. J.; Pople, J. A. *J. Chem. Phys.* **1982**, *77*, 3654.

(42) Ponder, W. J. Personal communication, 2004.

(43) Metropolis, N.; Rosenbluth, A. W.; Rosenbluth, M. N.; Teller, A. H.; Teller, E. *J. Chem. Phys.* **1953**, *21*, 1087.

(44) Parks, G. T. *Nucl. Technol.* **1990**, *89*, 233.

(45) Li, Z.; Scheraga, H. A. *Proc. Natl. Acad. Sci., U.S.A.* **1987**, *84*, 6611.

(46) Moller, C.; Plesset, S. *Phys. Rev.* **1934**, *46*, 618.

(47) Woon, D. E.; Dunning, T. H., Jr. *J. Chem. Phys.* **1993**, *98*, 1358.